

# Data, Depth, and Design: Learning Reliable Models for Melanoma Screening

Eduardo Valle\*, Michel Fornaciali, Afonso Menegola, Julia Tavares,  
Flávia Vasques Bittencourt, Lin Tzy Li, Sandra Avila

**Abstract**—State of the art on melanoma screening evolved rapidly in the last two years, with the adoption of deep learning. Those models, however, pose challenges of their own, as they are expensive to train and difficult to parameterize. **Objective:** We investigate the methodological issues for designing and evaluating deep learning models for melanoma screening, by exploring nine choices often faced to design deep networks: model architecture, training dataset, image resolution, type of data augmentation, input normalization, use of segmentation, duration of training, additional use of SVM, and test data augmentation. **Methods:** We perform a two-level full factorial experiment, for five different test datasets, resulting in 2560 exhaustive trials, which we analyze using a multi-way ANOVA. **Results:** The main finding is that the size of training data has a disproportionate influence, explaining almost half the variation in performance. Of the other factors, test data augmentation and input resolution are the most helpful. Deeper models, when combined, with extra data, also help. We show that the costly full factorial design, or the unreliable sequential optimization, are not the only options: ensembles of models provide reliable results with limited resources. **Conclusions and Significance:** To move research forward on automated melanoma screening, we need to curate larger shared datasets. Optimizing hyperparameters and measuring performance on the same dataset is common, but leads to overoptimistic results. Ensembles of models are a cost-effective alternative to the expensive full-factorial and to the unstable sequential designs.

**Index Terms**—Deep learning, melanoma screening, experimental design, model parametrization, cross dataset.

## I. INTRODUCTION

DEEP learning is today the gold standard for image classification. Automated melanoma screening is no exception, with a state of the art that improved rapidly in the last two years, since the adoption of those models.

However, deep learning poses challenges of its own, requiring great computational power and large amounts of annotated data. Deep learning is also challenging to parameterize, often involving dozens of hyperparameters [1]. Although high-level

frameworks have simplified its use, much craftsmanship is involved in designing and optimizing its models.

We examine those difficulties, with an exhaustive evaluation of nine choices often faced when designing deep networks for melanoma screening. We explore all variations of those factors in a two-level full factorial design, for five different test datasets, resulting in  $2^9 \times 5 = 2560$  experiments. We analyze those results using a multi-way ANOVA, to obtain decisions that generalize across datasets.

Full factorial designs are too expensive for most practical contexts, but the complete set of data we obtained allows us to simulate two alternative designs: the traditional sequential optimization (a single factor at a time) and ensembles of models. We show that the latter provides the best performance, at reasonable costs.

Our participation on the ISIC (International Skin Imaging Collaboration) 2017 Challenge [2], inspired the experiments in this paper. At the time, with a strategy of aggressively optimizing our models, we were ranked first in melanoma classification [3], with an AUC of 0.874. Here we have very different goals, focusing on methodological issues for designing and evaluating deep learning models for melanoma screening. We also show that the customary procedure of optimizing hyperparameters and evaluating techniques on the same dataset leads to overoptimistic results.

Our focus here is not getting the ultimate model, but examining those broader issues. We illustrate, however, that it is possible to follow the suggested procedure without incurring in performance penalties, by showcasing performances improved in comparison to our participation in the challenge.

We organized the remaining text as follows: we discuss the recent state of the art in Section II, and very briefly overview our participation on ISIC Challenge 2017. We detail our goals, materials, and methods in Section III. Experimental results and analyses appear in Section IV. Finally, we review and discuss the main findings in Section V.

## II. SURVEY OF RECENT TECHNIQUES

Since 2016, state of the art on automated melanoma took a sharp turn towards deep learning. We will focus on those results, without emphasis on relevant previous literature [4], [5], and refer the interested reader to more comprehensive surveys [6], [7]. We assume that the reader has passing familiarity with deep learning and its issues — if needed, we refer the reader to a complete overview [1].

E. Valle, M. Fornaciali, A. Menegola, and J. Tavares are affiliated to the Department of Computer Engineering and Industrial Automation (DCA) of the School of Electrical and Computing Engineering (FEEC), University of Campinas (UNICAMP), Campinas, Brazil.

E. Valle, M. Fornaciali, A. Menegola, J. Tavares, L. T. Li, and S. Avila are affiliated to the RECOD Lab.

J. Tavares is also affiliated to the Latam Experian DataLab, Sao Paulo, Brazil.

F. Bittencourt is affiliated to the School of Medicine, Federal University of Minas Gerais (UFMG), Belo Horizonte, Brazil.

L. T. Li is also affiliated to the Samsung Research and Development Institute Brazil, Campinas, Brazil.

S. Avila is affiliated to the Institute of Computing (IC), UNICAMP.

\*Contact author: dovalle@dca.fee.unicamp.br, mail@eduardovalle.com.

Existing works either train deep networks from scratch [8]–[10]; or reuse the weights from pre-trained networks [11]–[16], in a scheme called **transfer learning**.

Transfer learning is usually preferred, as it alleviates the main issue of deep learning for melanoma screening: way too small datasets — most often comprising a few thousand samples. (Contrast that with the ImageNet dataset, employed to evaluate deep networks, with more than *a million* samples.) Training from scratch is preferable only when attempting new architectures, or when avoiding external data due to legal/scientific issues. Menegola et al. [13] explain and evaluate transfer learning for automated screening in more detail. Here, all experiments employ transfer learning.

Whether using transfer or not, works vary widely in their choice of deep-learning architecture, from the relatively shallow (for today’s standards) VGG [11], [13], [14], [17], mid-range GoogLeNet [11], [12], [15], [18], [19], until the deeper ResNet [3], [15], [16], [20], [21] or Inception [3], [12], [22]. On the one hand, more recent architectures tend to be deeper, and to yield better accuracies; on the other hand, they require more data and are more difficult to parameterize and train. Although high-level frameworks for deep learning have simplified training those networks, a good deal of craftsmanship is still involved. In this work we contrast two architectures: **ResNet-101-v2** [23], and **Inception-v4** [24]. Both are very deep and show outstanding performance on ImageNet, but Inception-v4 is considerably deeper and bigger than ResNet-101-v2.

Data augmentation is another technique used to bypass the need for data, while also enhancing networks’ invariance properties. Augmentation creates a myriad of new samples by applying random distortions (e.g., rotations, crops, resizes, color changes) to the existing samples. Augmentation provides best performance when applied to both train and test samples, but only the most recent melanoma screening works follow that scheme [3], [9], [13], [21], [22]. Train-only augmentation is still very common [11], [12], [14], [17]–[19], [25].

In this work we evaluate two **augmentation distortion setups** (TensorFlow/Slim’s default for each network, and an attempt to customize it for skin lesions). We always apply augmentation to the training samples, but evaluate the impact of applying or not **augmentation for test samples**.

Works based on global features or bags of visual words often preprocess the images (some recent works using deep learning do it as well) to reduce noise, remove artifacts (e.g., hair), enhance brightness and color, or highlight structures [8], [10], [20], [26]–[28]. The deep-learning ethos usually forgoes that kind of “hand-made” preprocessing, relying instead on networks’ abilities to learn those invariances — with the help of data augmentation if needed.

On the other hand, segmentation as preprocessing is common on deep-learning for automated screening [9], [18], sometimes employing a dedicated network to segment the lesion before forwarding it to the classification network [11], [16], [25]. Those works usually report improved accuracies. In this work, we also evaluate the impact of **using segmentation** to help classification.

If ad-hoc preprocessing (e.g., hair removal) is atypical in deep-learning, *statistical* preprocessing is very common. Many networks fail to converge if the expected value of input data is too far from zero. Learning an average input vector during training set and subtracting it from each input is standard, and performing a comparable procedure for standard deviations is usual. The procedure is so routine, that with rare exceptions [3], [29], authors do not even mention it. In this work, we evaluate the impact of two **image normalization** schemes: TensorFlow/Slim’s default for each network, and an attempt to customize it for skin lesions.

Deep network architectures can directly provide the classification decisions, or can provide features for the final classifier — often support vector machines (SVM). Both the former [12], [14], [15], and the latter [8], [13], [16], [17] procedures are readily found for melanoma screening. We evaluate those **choices of adding or not an SVM layer**. Also common, are **ensemble techniques**, which fuse the results from several classifiers into a final decision [3], [15], [20]–[22].

As shown above, the literature on automated melanoma screening is vast: even the limited scope chosen for this survey comprises more than a dozen works. Making comparisons across those techniques was, until very recently, next to impossible due to poorly documented choices of datasets, splits, implementation details, or even evaluation metrics [7]. The ISIC Challenge [2] has sharply improved that scenario, by providing standards for data and metrics, and by requiring participants to publish working notes.

A subtler way ISIC Challenge served the community was by clearly separating validation and test datasets, and by keeping test datasets secret until all evaluations were over. When test sets are open, authors have an almost irresistible tendency to optimize hyperparameters on test (**hyperoptimize on test**, for short). Hyperoptimizing on test is *not* the same as *directly* contaminating training data with test samples — the latter is an obvious methodological blunder that most practitioners avoid, the former is much more subtle and much more frequent. It consists in attempting several choices of hyperparameters (network architectures, augmentation or transfer choices, training hyperparameters) and reporting those that performed best. That procedure, although very common, uses information from the test set (which should be treated as inaccessible) to make decisions about the model. As we will discuss, hyperoptimizing on test, leads to overoptimistic estimations of performance.

#### A. ISIC Challenge 2017

We documented our participation in Parts 1 and 3 of ISIC Challenge 2017 in our working notes [3]. In this section, we briefly summarize that participation, our findings, and contrast our aims then and now.

Our team has been working on melanoma classification since early 2014 [30], and has been employing deep learning with transfer learning for that task since 2015 [31]. On the other hand, we were tackling skin-lesion segmentation for the very first time. Our team reached 1st place in melanoma classification (AUC = 0.874), 3rd place at keratosis classification

(AUC = 0.943), and 3rd place in overall melanoma/keratosis classification (mean AUC = 0.908). We also reached 5th place in skin-lesion segmentation (Jaccard score = 0.754). The organizers published a comprehensive summary of the entire challenge [2].

The experiments presented here are inspired by the findings we made during the challenge, but this paper takes different directions, especially in terms of methodology. If during the challenge we tempered scientific rigor with the sportive desire to win, here we stress only the former: this work does not focus on maximizing AUCs, but on broader issues of experimental design and validation for the proposed methods.

### III. METHODS, DATA, AND MODELS

Our first — and more practical — goal is an exhaustive evaluation of nine factors involved in designing deep learning models:

- a Architecture of the deep-learning model;
- b Size/composition of the training dataset;
- c Resolution of the images on the training dataset;
- d Type of data augmentation;
- e (Statistical) normalization of the input data;
- f Use of lesion segmentation;
- g Duration of training;
- h Use of an additional SVM layer for the final decision;
- i Use of data augmentation on test samples.

Most of those factors are not particular to melanoma screening and must be considered for all image classifiers using deep learning. However, a preoccupation with resolution (c), augmentation customization (d), and segmentation (f) makes more sense for melanoma screening — or at least for medical images in general — than for general-purpose tasks, like ImageNet.

Our second, more philosophical, goal is a discussion of methodological issues in the design and evaluation of classification models, especially those which, like melanoma screening, aim at medical applications. We are far from the first to point out [32], [33] that the (very) usual practice of meta-optimizing a technique on the same test set used to evaluate the technique leads to over-optimistic results. In this paper, we showcase that effect as we cross-analyze the results in five different test sets.

#### A. Software and Hardware

We ran the experiments on a cluster of Ubuntu Linux machines, on a variety of NVIDIA GPUs, including Titan X Maxwell, Titan X Pascal, and Tesla K40. The classification models were built over Python/TensorFlow v.1.3. using the Slim framework. Slim provides ready-to-use models for ResNet-101-v2 and Inception-v4, which we used, with slight adaptations. The statistical analysis ran in R.

In this text we aimed to provide the details needed to understand all results; for complete reproducibility we provide the end-to-end pipeline, from the raw data to the tables and figures, at our code repository<sup>1</sup>.

<sup>1</sup><https://github.com/learningtitans/isbi2017-part3>, currently with the code used for the ISIC 2017 challenge.

#### B. Experimental Design

The main experimental design was a two-level full factorial design for all 9 factors mentioned above, for each one of the five test datasets, resulting in  $2^9 \times 5 = 2560$  experiments performed. In all experiments, we used the area under the Receiver Operating Characteristic curve (AUC) as main metric. Following the ISIC Challenge 2017, we use the mean AUC between the melanoma-vs-all and the keratosis-vs-all as the measured outcome in all experiments.

The main analysis was a classical multi-way ANOVA, in which the test datasets entered as one of the factors. That choice highlights our aim to make decisions that generalize across datasets, in contrast to maximizing the performance for a particular dataset.

ANOVA provides both a significance analysis (p-value), and a partition of the variance, which allows to roughly estimate the relative importance/influence of each factor, or combinations of factors. For effect size/explanatory power, we use the  $\eta^2$  measure, which is the ratio of the variances (sums-of-squares), extensively used due to its simplicity. The ANOVA table is summarized in Table II and explored in the next section. We also employed correlograms to highlight issues relating to the choice of test dataset, and performance metric (Fig. 1).

Most of the time, our full factorial designs are too costly to use — thus our next set of experiments, exploring ensemble techniques, helps in more practical situations. We evaluated a straightforward ensemble, which just pools the decision of several classifiers, and showed that it provides very good performances, without the costs of a full design.

We also simulated the most common procedure employed by researchers and practitioners: sequential optimization of hyperparameters, in which one starts from a given configuration of hyperparameters, selects one of them to evaluate, commits to the best results, and proceeds to evaluate the next. Although such procedure is very fast (it allows optimizing our 9 factors in just 18 experiments), it is sub-optimal in comparison to ensembles.

Finally, we showed that the customary procedure of optimizing the hyperparameters in the same test set used to evaluate the technique leads to overoptimistic results in both the ensemble and the sequential design.

Details and results of all procedures appear in Section IV.

#### C. Data

Due to deep-learning greediness for data, we sought all high-quality publicly available (for free, or for a fee) sources to compound our dataset:

- 1) *ISIC 2017 Challenge* [2], the official challenge dataset, with 2,000 dermoscopic images (374 melanomas, 254 seborrheic keratoses, and 1,372 benign nevi).
- 2) *ISIC Archive*, with over 13,000 dermoscopic images.
- 3) *Dermofit Image Library* [34], with 1,300 clinical images (76 melanomas, 257 seborrheic keratoses).
- 4) *PH2 Dataset* [35], with 200 dermoscopic images (40 melanomas).



TABLE I  
SUMMARY OF THE TRAIN AND TEST SETS.

Type	Melanoma	Nevus	Keratosis
ISIC Challenge 2017 train split	374	1372	254
Full train (composition of datasets)	1227	10124	710
Internal test split from full	135	3129	89
ISIC Challenge 2017 validation split	30	78	42
ISIC Challenge 2017 testing split	117	393	90
EDRA Atlas of Dermoscopy (each version)	518	1154	95

- 5) *EDRA Interactive Atlas of Dermoscopy* [36], with 1,000+ clinical cases (270 melanomas, 49 seborrheic keratoses), each with at least two images (dermoscopic, and close-up clinical).

We used essentially the same data sources we employed during the ISIC 2017 challenge, except the IRMA Dataset, because of the difficulties faced by other researchers to obtain it. Even with that exclusion, the new dataset grew, due to a more careful matching of diagnostics among the sources (instead of dropping the doubtful cases).

Besides this matching, which we performed with a thesaurus of the terms used in the different datasets, we also annotated images by case, by aliases (same image with different names), and by near-duplicates (two almost-copies of the same lesion). When creating the train and test sets, we barred any cases, aliases, or near-duplicates from splitting across sets.

Data sources affect the train and test datasets. For the train dataset (factor b), we contrasted (1) using only the official training split of the ISIC Challenge 2017 dataset, to (2) joining the training split of the ISIC Challenge, the ISIC Archive, the Dermofit Library, and the PH2 Dataset and extracting from that full dataset a training split. For the test dataset (factor j), we contrasted (1) an internal test split extracted from our full dataset; (2) the official validation split and (3) the official test split of ISIC Challenge 2017; (4) the dermoscopic images and (5) the clinical images of the EDRA Interactive Atlas of Dermoscopy. Table I summarizes the final assembled sets.

#### D. Models

In all experiments, we employed pre-trained models that proved successful for the ImageNet task. To evaluate the choice of the model (factor a) we contrasted two architectures: ResNet-101-v2 [23], and Inception-v4 [24], using the reference implementation available in TensorFlow/Slim v1.3.

In this paper, segmentation was used only as an ancillary input for classification (factor f). For the ISIC Challenge 2017, we had used a segmentation network based on the work of Ronneberger et al. [37] and Codella et al. [38]. For this work, we streamlined that model, reducing the number of parameters, removing the fully-connected and Gaussian-noise layers, and adding batch-normalization and dropout layers. The new model<sup>2</sup> is faster to train and occupies much less disk space. The segmentation models were trained on the same images as their corresponding classification models.

<sup>2</sup><https://github.com/learningtitans/isbi2017-part1>, currently with the code used for the ISIC 2017 challenge

For the experiments involving segmentation, we had to modify ResNet and Inception, by adding adapter layers that receive four planes as input (the RGB planes and the segmentation mask) and output only three planes, as expected by the original networks. For both ResNet/Inception we added three convolutional layers before the input, two layers with 32 filters, and a third with 3 filters. All convolutional layers used  $3 \times 3$  kernels and stride of 1. Since ResNet-101-v2 and Inception-v4 models require input images of  $299 \times 299$  pixels, the adapter layer took  $305 \times 305$ -pixel images, to account for the 2 border pixels lost at each convolutional layer.

#### IV. EXPERIMENTS

As explained, the main experiment was a full factorial design with nine two-level factors, and five test datasets. We used a classical multi-way ANOVA with the mean AUC for melanoma and keratosis as the measured outcome (with the small technicality of taking the logit of that measure, since, when working with rates, the logit helps to fulfill ANOVA's assumption of Gaussian residuals). We considered all main effects, and up to 3-way interactions. We considered higher-order interactions unlikely and assigned them to the model residuals.

Table II shows a summary of ANOVA results, with the symbols for the factors and interactions on the first column, and the names of the main factors on the second. The remaining columns show the outcomes of the test. The most important columns are *p-value*, which measures statistical significance, and *explanation (%)*, which measures effect-size/explanatory power. The p-value is inferred, as usual, from the F-statistic of ANOVA, while the explanatory power uses the  $\eta^2$  measure. We present the absolute explanation (considering the entire table) for reference, but our analysis is focused on the relative explanation, which ignores the choice of the test set (j) and the residuals. The reason for ignoring those is that they are not actual choices for designing a new model; therefore, relative explanations indicate better the relative importance of choices to practitioners.

The original full table contained all main effects, and up to 3-way interactions. However, not surprisingly, 126 of the resulting 176 lines were non-significant interactions, which were omitted here. We also left out those interactions with relative explanations lower than 1%, even if significant. With the notable exception of the customized data augmentation (d), all main effects were significant, but most of their relative explanations were small.

The analysis of the relative explanation shows an unsurprising, but still disappointing result: the performance gains (b) are almost wholly due to the usage of more data. Other than data, the most important factor was the use of data augmentation on test (d). We performed it, as usual, by taking the test image, generating a number (in our case, 50) of augmented samples exactly like in training, collecting the prediction for each of the samples, and pooling the decisions (in our case, by taking the average prediction). Although not surprising for the literature of deep learning, that finding is relevant for the literature of melanoma screening, where many works still forgo augmentation in the test.

TABLE II

SELECTED LINES FROM THE 176-LINE ANOVA TABLE; MOST OF THE OMITTED LINES (126) HAD P-VALUES  $\geq 0.05$ . ABSOLUTE EXPLANATION BASED ON  $\eta^2$ -MEASURE, RELATIVE EXPLANATION IGNORES RESIDUALS AND CHOICE OF TEST DATASET (J).

			Explanation (%)		Best AUC (%)		Worst AUC (%)	
	Factor	p-value	Absolute	Relative	Treatment	Mean	Treatment	Mean
a	Model architecture	<0.001	0	1	resnet	84	inception	83
b	Train dataset	<0.001	5	46	full	85	isic	81
c	Input resolution	<0.001	1	5	598	84	299	82
d	Data augmentation	0.17	0	0	default	83	custom	83
e	Input normalization	0.001	0	0	yes	83	no	83
f	Use of segmentation	<0.001	0	2	no	84	yes	83
g	Duration of training	0.003	0	0	full	83	half	83
h	SVM layer	<0.001	0	4	no	84	yes	83
i	Augmentation on test	<0.001	1	12	yes	84	no	82
j	Test dataset	<0.001	75		int. split	96	edra.clinic.	66
a:b		<0.001	1	8	incep/full	86	incep/isic	80
a:f		<0.001	0	2	resnet/no	84	incep/yes	82
b:e		<0.001	0	2	full/no	86	isis/no	80
b:j		<0.001	2		full/int.	98	isic/edra.clin	63
h:j		<0.001	0		no/int.	97	yes/edra.clin	65
i:j		<0.001	0		yes/int.	97	no/edra.clin	65
a:b:d		<0.001	0	2	incep/full/custom	86	incep/isic/custom	78
a:d:e		<0.001	0	2	resnet/custom/no	85	incep/custom/no	81
a:f:j		<0.001	0		resnet/yes/int.	97	incep/yes/edra.clin	65
b:d:e		<0.001	0	1	full/custom/no	86	isic/custom/no	79
c:e:f		<0.001	0	1	598/yes/no	86	299/no/yes	82
Residuals		—	12					

Most of the findings tended to confirm the (limited) observations we made during the ISIC Challenge 2017, with two notable exceptions. Input resolution (c), which we deemed unimportant during the challenge, turned out to have a non-negligible effect. That result is particularly interesting, because we used a very rough form of augmented resolution, by inputting high-resolution images to the augmentation engine, but still feeding normal-resolution crops to the network. On the other hand, the use of an SVM decision layer (h), which we considered advantageous during the Challenge turned out to have a large-effect... only negative! Globally, ANOVA shows it is better *not* to use the SVM.

Normalization (e) and training duration (g) showed tiny (<1%), but still significant positive effects. The choice for those factors must consider their very different costs: adding normalization costs next to nothing, both in implementation complexity and in training time. Training duration doubled the already many-hours-long training times.

As usual, most of the interactions were not significant, and even the ones that were, had effect sizes too small to be worth noting. A notable exception was the interaction between model architecture and train dataset (a:b), whose 8% of relative explanation was bigger than most main effects. Model choice alone favors the simplest ResNet over Inception, but the combination of Inception with the full dataset is so advantageous that it offsets that effect. We had already observed, informally, this synergy between more data and deeper models during the Challenge.

The most disappointing result was the use of segmentation, which was more than unhelpful, harmful. We did (separate) preliminary tests on two ways of incorporating segmentation on the deep networks: pre-applying the segmentation masks to the RGB images and inputting the transformed images to the

usual networks, or adapting the networks to receive four planes (R, G, B, and mask) instead of three. For the full design, we only considered the latter, which proved most promising on those preliminary results.

We performed an additional correlation analysis with the full factorial experiment (Fig. 1), to highlight the correlations (a) among results on different test datasets; and (b) among different metrics. To keep the scatter plots directly interpretable, instead of taking the logit of the rates, we dealt with the non-linearity by using Spearman's  $\rho$  instead of Pearson's  $r$  as correlation measure.

The correlogram on Fig. 1a considers, as the ANOVA, the mean melanoma/keratosis AUC. The test dataset names appear in the diagonal, along with the maximum and minimum AUCs obtained for the 512 variations of the full design on that dataset. The scatter plots in the upper-triangular matrix follow the usual construction for correlograms. The lower-triangular matrix displays the Spearman's  $\rho$ 's: the mean estimate appears as the printed numeral and as the area of the solid circle; the bounds of the 95%-confidence interval appear as the area of the internal and external dashed circles. Negative correlations appear in red.

The correlation between different test datasets is far from perfect. That is, perhaps, obvious, but must be stressed, since it reveals that *naively* hyperoptimizing a model on one test set will not necessarily generalize to other data. The relationship between splits of different datasets is more subtle. Note how the correlation between the validation and the test splits of ISIC 2017 Challenge, and the dermoscopic and clinical splits of EDRA have the highest correlations. This suggests that results measured on splits of the same dataset may not wholly generalize over data of the same type obtained on different conditions. Both phenomena show how hyperoptimizing on

test gives unwarranted advantages, leading to overoptimistic assessments.

The correlogram on Fig. 1b considers only the results on the test split of the ISIC Challenge. Different metrics are shown in the diagonal: average precision, area under the ROC curve, sensitivity (true positive rate), and specificity (true negative rate), for both melanoma and keratosis. The interpretation of the plots, numerals, circles, and colors is the same as above.

This correlogram is interesting for showing that many metrics have correlations that are not that big. Particularly noteworthy is the specificity, which has not only a negative correlation with sensitivity (as expected), but also a negative or very small correlation with *most of* the other metrics.

As mentioned, full factorial designs are way too expensive for the majority of situations. The most common procedure is the exact opposite: taking a single factor to optimize, and performing a couple of experiments on that factor alone, keeping all others fixed (starting from a combination considered reasonable). Once a factor is decided, one commits to it and takes the next to optimize, until the procedure is complete.

We evaluate the impact of such sequential procedure, simulating it using the measurements on the full design. We take, at random, both the starting treatment and the sequence of factors to test. For factors not yet optimized, the level is given by the starting treatment. Each factor is optimized in turn, by comparing the performance of the alternative treatments on the full-factorial data of a chosen hyperoptimization dataset. The outcome of a single simulation is the performance of the optimized treatment on a chosen measurement dataset. We use the mean keratosis/melanoma AUC as the performance metric.

Fig. 2 shows the results for pairs of hyperoptimization  $\times$  measurement datasets, where we perform 100 simulations for each pair. The most notable observation is the (unrealistic) advantage of hyperoptimizing and measuring on the same dataset: not only do we get higher averages, but also a smaller variability. The advantage of hyperoptimizing and measuring on splits of the same dataset is more subtle, but present.

The expense of the full factorial design, the instability of the sequential procedure, and the limited correlation of performances across datasets seem to leave few options to practitioners. Fortunately, single-model schemes are seldom used today, and an ensemble of several models help to alleviate those issues.

We simulated different ensemble strategies, by pooling the predictions of models present in our full design. We evaluate three pooling strategies: average, max, and extremal. Average- and max-pooling work as usual. Extremal pooling takes, from the list of values being pooled, the value most distant from 0.5 — it may be seen as an “hypothesis-invariant” max-pooling. In all cases, after pooling, we re-normalize the probability vector to ensure it sums up to one. Half the models in the full design entered as candidates, and we discarded in this experiment the models with the SVM layer, due to issues in making their probabilities commensurable with the deep-only models.

Fig. 3 shows the main results. Average pooling was, by far, the best choice for pooling the decision. Such clear-cut advantage came as a surprise for us, as max pooling often outperforms average pooling in related tasks. If no other

information is available, simply average-pooling randomly selected models is a reasonable strategy.

The use of dozens — even hundreds — of models may sometimes be justified in critical tasks (like medical decisions), but training and evaluating so many deep networks is cumbersome. Fortunately, as Fig. 4 shows, a handful of models seem to work just as well. The results shown here are the “good news” part of this paper: we can escape the expense of the full factorial design, and the instability of the sequential designs, by averaging a dozen or so models with parameters chosen entirely at random — although the random ensembles start very unstable, they soon converge to a reasonable model, in average and variability. If we decide to perform a full factorial, there is good news too: the best models learned in one dataset seem to be informative to compose the ensembles in other datasets, allowing to get top performances with very small ensembles.

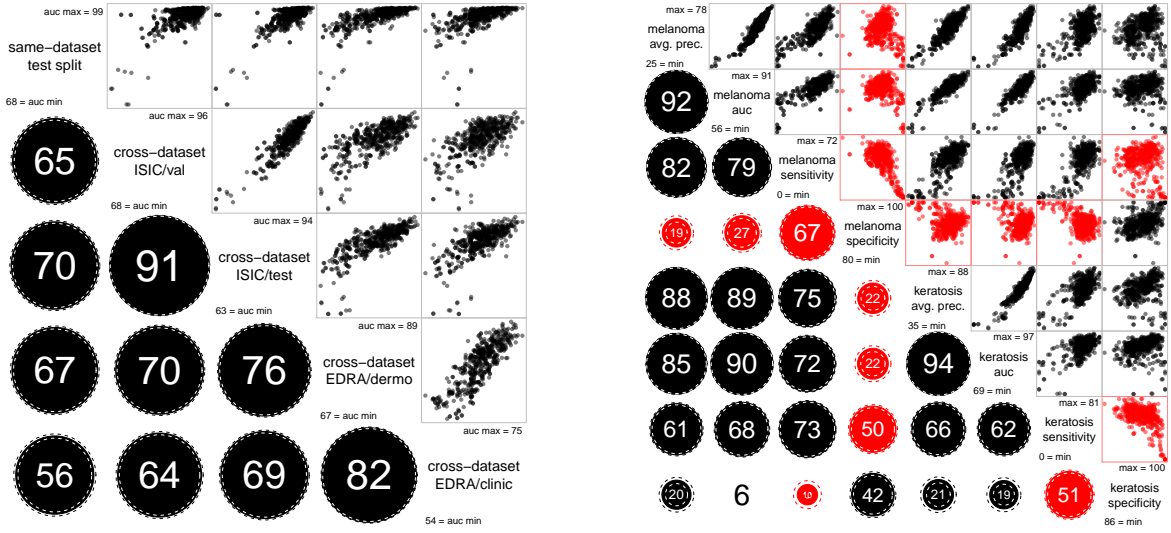
Here, again, the unfair advantage of optimizing (selecting the models for the ensemble) and measuring performance on the same dataset appears. The advantage is small but systematic for the test split of ISIC (Fig. 4a); it is much more apparent for the challenging collection of clinical images of EDRA Atlas (Fig. 4b).

As a final experiment, we made two simulations of “new” submissions to the ISIC 2017 Challenge. The first simulates a *blind* procedure, mimicking the conditions of the challenge (limited information about the validation split, no information whatsoever about the test split). In that simulation, we assume a full factorial experiment performed only on our internal validation split, and keep the 32 best models (as measured in that split). We then test 32 incremental ensembles on the ISIC validation set, finding that the ensembles with 15 or 16 models have the best performance. We commit to the ensemble with 15 models and do *one* evaluation of that ensemble on the ISIC test split, finding AUCs of 0.895 (melanoma), 0.967 (keratosis), and 0.931 (combined). To put those numbers in perspective, in the actual competition the best AUCs were, respectively, 0.874, 0.965, and 0.911 (obtained by different participants).

We also simulated a *privileged* procedure, hyperoptimizing without restraint on the ISIC Challenge test split itself. We use the full design on the ISIC Test split to select the 32 best models, and then test 32 incremental ensembles, handpicking the best result for melanoma and for keratosis. We find AUCs of 0.916 (melanoma), 0.970 (keratosis), and 0.943 (combined). Again, to get a better grasp of the difference, consider that the 2.p.p. increase on the melanoma AUCs is larger than the difference between the 1st and the 4th teams ranked in the 2017 Challenge.

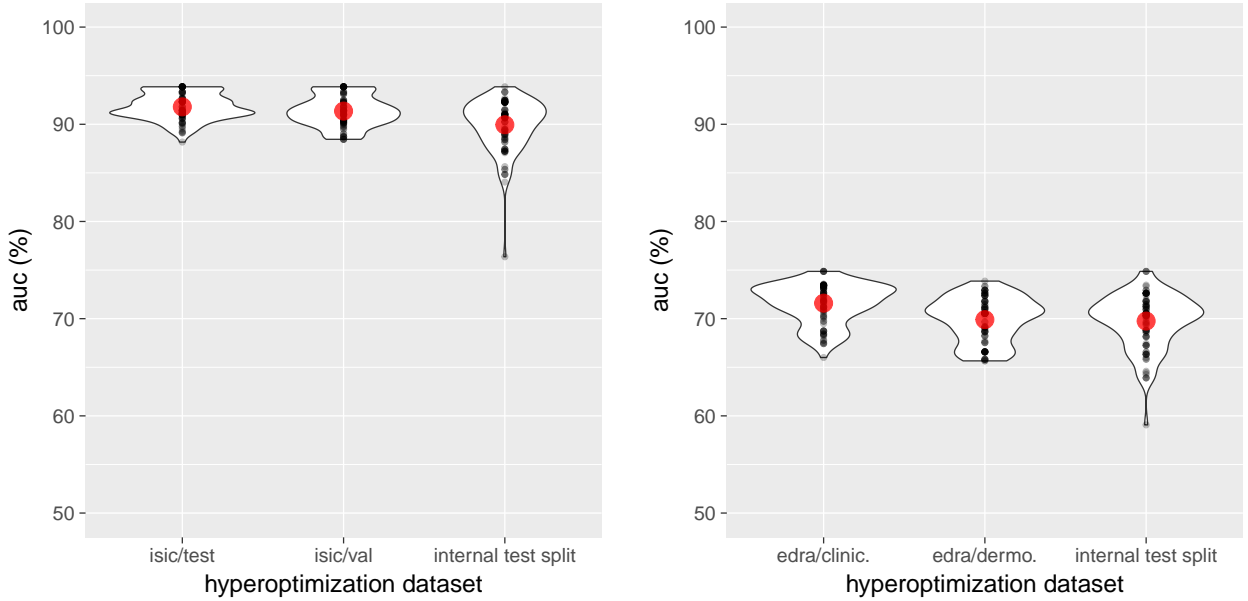
## V. DISCUSSION

When one contrasts the blind and the privileged procedures side-by-side, the problems with the latter become apparent, but the privileged protocol is the most common in machine-learning literature (we are often guilty ourselves). Hyperoptimizing on test does not result from researchers’ desire to cheat, but from their natural tendency to exploit scarce existing data



(a) Correlogram of mean melanoma/keratosis AUC across test datasets. (b) Correlogram of metrics on ISIC 2017 Test dataset across metrics.

Fig. 1. Correlograms with pair-wise correlation analyses. Sets appear on the diagonal; upper matrices show the scatter plots, and lower matrices show the Spearman correlation of each pair of sets. On lower matrices, numbers and solid circles' areas show the mean estimates, and dashed circles' areas show the 95%-confidence bounds. Non-significant estimates appear without the circles. All numbers in %, negative correlations are in red.



(a) Simulated sequential design on ISIC test split.

(b) Simulated sequential design on EDRA Atlas clinical images.

Fig. 2. Simulation of the sequential optimization of hyperparameters, considering all nine factors (a-i) as the full factorial. Factors optimized on the dataset shown on the horizontal axis, and performance (mean melanoma/keratosis AUC) measured on the dataset indicated on the captions. For each case, we run 100 simulations (black dots), with random optimization sequences and starting points. The violin plots show the estimated density, and the large red dot shows the mean.

as much as possible. Salzberg has warned authors about the dangers of “repeated tuning” since 1997; his work [32] is often cited, but the issue is still far from solved.

Avoiding that pitfall requires a very strong commitment, which researchers seem unable to keep. That only reinforces the importance of regular curated challenges — like the ISIC

Challenge — in which the test set is withheld at least until the evaluations are over. The ImageNet competition is perhaps the best example of the extraordinary impact of having such a curated competition every year.

Our findings explain, in part, why performances observed in practice fall much shorter of the numbers we get in our labs.

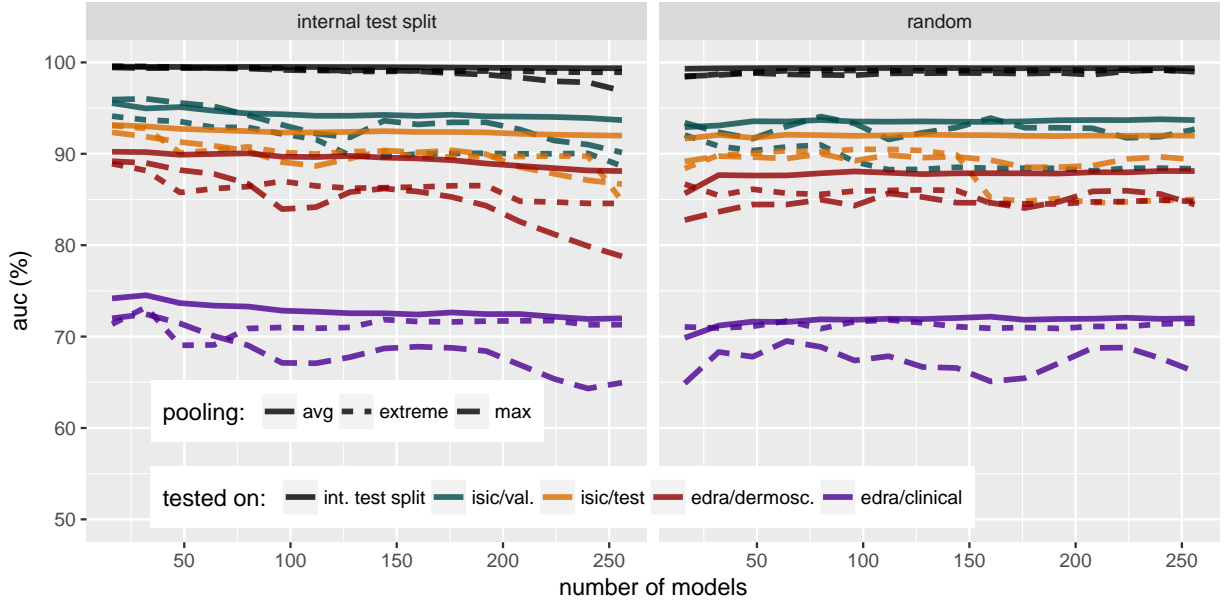
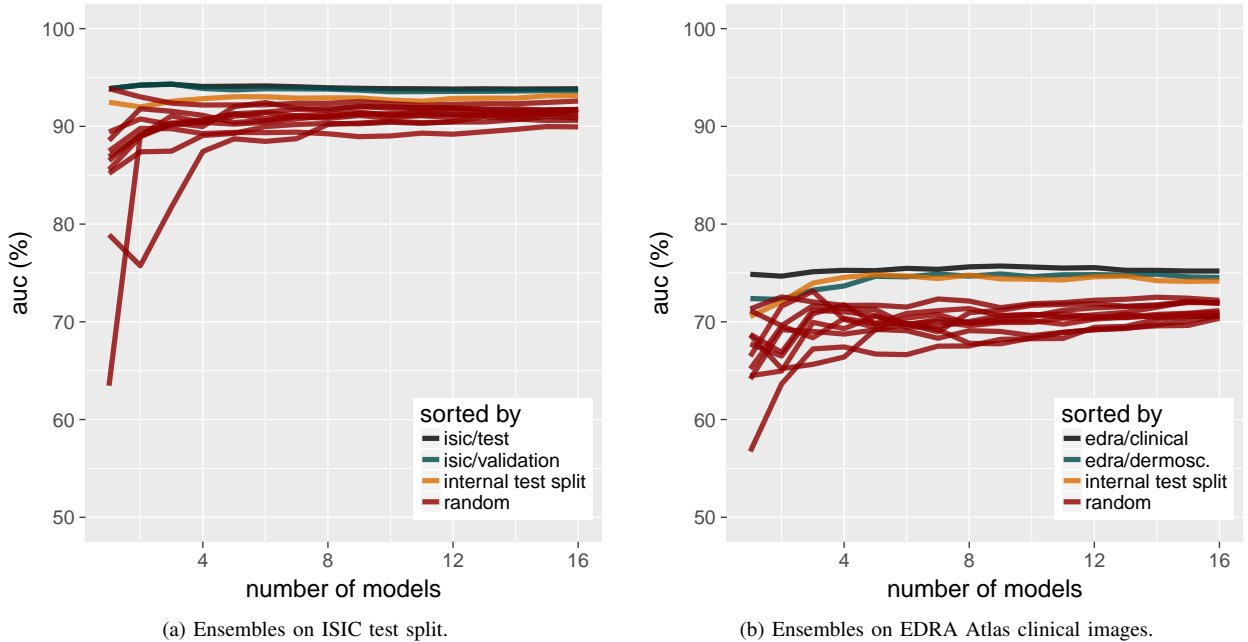


Fig. 3. Evaluation of ensemble strategies, by pooling the prediction of a given number of partial models using average-, max-, or extremal-pooling. Left: cumulative effect of adding partial models, starting with the best (as evaluated by the internal test split). Right: same plot, with models randomly shuffled. (Best viewed in color.)



(a) Ensembles on ISIC test split.

(b) Ensembles on EDRA Atlas clinical images.

Fig. 4. Detailed analysis of ensembles, contrasting the dataset used to choose the models (shown as different curves) in order to optimize the results for a measurement dataset (indicated in captions). We sampled 10 different random ensembles. (Best viewed in color.)

In a single round of experiments, analyzing only two levels for nine factors, the unwarranted advantage of hyperoptimizing on test is already notable. In actual research, with many rounds of experiments over dozens of factors and hundreds of levels, the gap may be much wider.

Our evaluation of 2560 different models shows that almost half the variability in performance is explained by the amount of data alone. That reinforces the deep-learning creed on the “unreasonable power of data” and has important consequences

for the melanoma screening community: in order to move research forward, we need to curate larger shared datasets. The ISIC Archive is an essential step in that direction — but it would have to grow almost tenfold to match the largest (private) dataset reported in the literature [12].

Despite the predominance of data, other factors appeared relevant. The most noteworthy is, perhaps, the use of data augmentation on test samples. The use of deeper models *in combination* with extra data, also appeared as an important



advantage. Increased resolution — even in a very limited scheme — was also advantageous.

Notable *negative* results were the use of segmentation to help classification, and the use of an extra SVM Layer. The negative result on segmentation is the most surprising, and needs further exploration, since so many works in literature report improved performances.

The limited correlation between different possible metrics (in particular with specificity) has consequences for melanoma screening literature: stressing one metric over the other may lead the community to different directions.

The ensemble experiments bring the most encouraging news, by providing reliable performance, without either the expense of the full factorial design, or the instability of the traditional sequential optimization. Even a simple accumulation of enough randomly-sampled models was sufficient to provide adequate performance. Learning the best models on one dataset, however, helps to select the best ensembles for other datasets.

Ensembles appear as a promising avenue for future explorations. In future works, we would like to design and evaluate techniques more sophisticated than pooling the decisions of the models, like model stacking, or boosting.

#### ACKNOWLEDGMENT

E. Valle and M. Fornaciali are partially funded by Google Research Awards for Latin America 2016 & 2017; E. Valle is also partially funded by a CNPq PQ-2 grant (311486/2014-2). A. Menegola is funded by CNPq. This project is partially funded by CNPq Universal grant (424958/2016-3). RECOD Lab. is partially supported by diverse projects and grants from FAPESP, CNPq, and CAPES. We gratefully acknowledge the donation of a Tesla K40 and a TITAN X GPUs by NVIDIA Corporation, used in this work. We thank Fabio Perez and Micael Carvalho for the final revision. We thank Prof. M. Emre Celebi for kindly providing the machine-readable metadata of the EDRA Interactive Atlas of Dermoscopy and for the help with the final revision.

#### REFERENCES

- [1] Y. LeCun, Y. Bengio, and G. Hinton, "Deep learning," *Nature*, vol. 521, no. 7553, pp. 436–444, 2015.
- [2] N. C. Codella, D. Gutman, M. E. Celebi, B. Helba, M. A. Marchetti, S. W. Dusza, A. Kalloo, K. Liopyris, N. Mishra, H. Kittler *et al.*, "Skin Lesion Analysis Toward Melanoma Detection: A Challenge at the 2017 International Symposium on Biomedical Imaging (ISBI), Hosted by the International Skin Imaging Collaboration (ISIC)," *arXiv preprint arXiv:1710.05006*, 2017.
- [3] A. Menegola, J. Tavares, M. Fornaciali, L. T. Li, S. Avila, and E. Valle, "RECOD Titans at ISIC Challenge 2017," *arXiv preprint arXiv:1703.04819*, 2017.
- [4] M. E. Celebi, H. A. Kingravi, B. Uddin, H. Iyatomi, Y. A. Aslandogan, W. V. Stoecker, and R. H. Moss, "A methodological approach to the classification of dermoscopy images," *Computerized Medical Imaging and Graphics*, vol. 31, no. 6, pp. 362–373, 2007.
- [5] H. Iyatomi, H. Oka, M. E. Celebi, M. Hashimoto, M. Hagiwara, M. Tanaka, and K. Ogawa, "An improved internet-based melanoma screening system with dermatologist-like tumor area extraction algorithm," *Computerized Medical Imaging and Graphics*, vol. 32, no. 7, pp. 566–579, 2008.
- [6] G. Litjens, T. Kooi, B. E. Bejnordi, A. A. A. Setio, F. Ciompi, M. Ghafoorian, J. A. der Laak, B. G. Clara, and I. Sánchez, "A survey on deep learning in medical image analysis," *Medical Image Analysis*, vol. 42, pp. 60–88, 2017.
- [7] M. Fornaciali, M. Carvalho, F. V. Bittencourt, S. Avila, and E. Valle, "Towards automated melanoma screening: Proper computer vision & reliable results," *arXiv preprint arXiv:1604.04024*, 2016.
- [8] S. Sabbaghi, M. Aldeen, and R. Garnavi, "A deep bag-of-features model for the classification of melanomas in dermoscopy images," in *IEEE Engineering in Medicine and Biology Society*, 2016, pp. 1369–1372.
- [9] E. Nasr-Esfahani, S. Samavi, N. Karimi, S. M. R. Soroushmehr, M. H. Jafari, K. Ward, and K. Najarian, "Melanoma detection by analysis of clinical images using convolutional neural network," in *IEEE Engineering in Medicine and Biology Society*, 2016, pp. 1373–1376.
- [10] X. Jia and L. Shen, "Skin lesion classification using class activation map," *arXiv preprint arXiv:1703.01053*, 2017.
- [11] L. Yu, H. Chen, Q. Dou, J. Qin, and P.-A. Heng, "Automated melanoma recognition in dermoscopy images via very deep residual networks," *IEEE Transactions on Medical Imaging*, vol. 36, no. 4, pp. 994–1004, 2017.
- [12] A. Esteva, B. Kuprel, R. A. Novoa, J. Ko, S. M. Swetter, H. M. Blau, and S. Thrun, "Dermatologist-level classification of skin cancer with deep neural networks," *Nature*, vol. 542, no. 7639, pp. 115–118, 2017.
- [13] A. Menegola, M. Fornaciali, R. Pires, F. V. Bittencourt, S. Avila, and E. Valle, "Knowledge transfer for melanoma screening with deep learning," in *IEEE International Symposium on Biomedical Imaging*, 2017, pp. 297–300.
- [14] A. R. Lopez, X. Giro-i Nieto, J. Burdick, and O. Marques, "Skin lesion classification from dermoscopic images using deep learning techniques," in *IEEE International Conference on Biomedical Engineering (BioMed)*, 2017, pp. 49–54.
- [15] B. Harangi, "Skin lesion detection based on an ensemble of deep convolutional neural network," *arXiv preprint arXiv:1705.03360*, 2017.
- [16] N. C. Codella, Q.-B. Nguyen, S. Pankanti, D. Gutman, B. Helba, A. Halpern, and J. R. Smith, "Deep learning ensembles for melanoma recognition in dermoscopy images," *IBM Journal of Research and Development*, vol. 61, no. 4, pp. 5:1–5:15, 2017.
- [17] Z. Ge, S. Demyanov, B. Bozorgtabar, M. Abedini, R. Chakravorty, A. Bowling, and R. Garnavi, "Exploiting local and generic features for accurate skin lesions classification using clinical and dermoscopy imaging," in *IEEE International Symposium on Biomedical Imaging (ISBI)*, 2017, pp. 986–990.
- [18] X. Yang, Z. Zeng, S. Y. Yeo, C. Tan, H. L. Tey, and Y. Su, "A novel multi-task deep learning model for skin lesion segmentation and classification," *arXiv preprint arXiv:1703.01025*, 2017.
- [19] C. N. Vasconcelos and B. N. Vasconcelos, "Increasing deep learning melanoma classification by classical and expert knowledge based image transforms," *arXiv preprint arXiv:1702.07025*, 2017.
- [20] K. Matsunaga, A. Hamada, A. Minagawa, and H. Koga, "Image classification of melanoma, nevus and seborrheic keratosis by deep neural network ensemble," *arXiv preprint arXiv:1703.03108*, 2017.
- [21] L. Bi, J. Kim, E. Ahn, and D. Feng, "Automatic skin lesion analysis using large-scale dermoscopy images and deep residual networks," *arXiv preprint arXiv:1703.04197*, 2017.
- [22] T. DeVries and D. Ramachandram, "Skin lesion classification using deep multi-scale convolutional neural networks," *arXiv preprint arXiv:1703.01402*, 2017.
- [23] K. He, X. Zhang, S. Ren, and J. Sun, "Identity mappings in deep residual networks," in *European Conference on Computer Vision*, 2016, pp. 630–645.
- [24] C. Szegedy, S. Ioffe, V. Vanhoucke, and A. A. Alemi, "Inception-v4, inception-resnet and the impact of residual connections on learning," *AAAI Conference on Artificial Intelligence*, pp. 4278–4284, 2017.
- [25] I. G. Díaz, "Incorporating the knowledge of dermatologists to convolutional neural networks for the diagnosis of skin lesions," *arXiv preprint arXiv:1703.01976*, 2017.
- [26] Q. Abbas, M. Emre Celebi, I. F. Garcia, and W. Ahmad, "Melanoma recognition framework based on expert definition of abcd for dermoscopic images," *Skin Research and Technology*, vol. 19, no. 1, 2013.
- [27] P. Wighton, T. K. Lee, H. Lui, D. I. McLean, and M. S. Atkins, "Generalizing common tasks in automated skin lesion diagnosis," *IEEE Transactions on Information Technology in Biomedicine*, vol. 15, no. 4, pp. 622–629, 2011.
- [28] T. Yoshida, M. E. Celebi, G. Schaefer, and H. Iyatomi, "Simple and effective pre-processing for automated melanoma discrimination based on cytological findings," in *IEEE International Conference on Big Data*, 2016, pp. 3439–3442.
- [29] J. Kawahara, A. BenTaieb, and G. Hamarneh, "Deep features to classify skin lesions," in *IEEE International Symposium on Biomedical Imaging*, 2016, pp. 1397–1400.

- [30] M. Fornaciali, S. Avila, M. Carvalho, and E. Valle, "Statistical learning approach for robust melanoma screening," in *Conference on Graphics, Patterns and Images (SIBGRAPI)*, 2014, pp. 319–326.
- [31] M. Carvalho, "Transfer schemes for deep learning in image classification," Master's thesis, University of Campinas, 2015.
- [32] S. L. Salzberg, "On comparing classifiers: Pitfalls to avoid and a recommended approach," *Data Mining and Knowledge Discovery*, vol. 1, no. 3, pp. 317–328, 1997.
- [33] A. Torralba and A. A. Efros, "Unbiased look at dataset bias," in *IEEE Conference on Computer Vision and Pattern Recognition*, 2011, pp. 1521–1528.
- [34] L. Ballerini, R. B. Fisher, B. Aldridge, and J. Rees, "A color and texture based hierarchical K-NN approach to the classification of non-melanoma skin lesions," in *Color Medical Image Analysis*, 2013, pp. 63–86.
- [35] T. Mendonça, P. M. Ferreira, J. S. Marques, A. R. Marcal, and J. Rozeira, "PH2 A dermoscopic image database for research and benchmarking," in *IEEE Engineering in Medicine and Biology Society*, 2013, pp. 5437–5440.
- [36] G. Argenziano, H. P. Soyer, V. De Giorgi, D. Piccolo, P. Carli, M. Delfino *et al.*, "Dermoscopy: a tutorial," *EDRA, Medical Publishing & New Media*, 2002.
- [37] O. Ronneberger, P. Fischer, and T. Brox, "U-Net: Convolutional networks for biomedical image segmentation," in *Medical Image Computing and Computer Assisted Intervention*, 2015, pp. 234–241.
- [38] N. Codella, J. Cai, M. Abedini, R. Garnavi, A. Halpern, and J. R. Smith, "Deep learning, sparse coding, and svm for melanoma recognition in dermoscopy images," in *International Workshop on Machine Learning in Medical Imaging*, 2015, pp. 118–126.